Colloids and Surfaces A: Physicochemical and Engineering Aspects 625 (2021) 126993

Contents lists available at ScienceDirect

Colloids and Surfaces A: Physicochemical and Engineering Aspects

journal homepage: www.elsevier.com/locate/colsurfa

High energy density in poly(vinylidene fluoride-trifluoroethylene) composite incorporated with modified halloysite nanotubular architecture

Ye Tian [a,b], Qiangqiang Qian [a,b], Yufeng Sheng [a,b], Xuanhe Zhang [c], Huaping Wu [a,b,*], Lixin Xu [c], Long Li [d,**], Huijian Ye [c,**]

[a] College of Mechanical Engineering, Zhejiang University of Technology, Hangzhou 310023, China
[b] Key Laboratory of Special Purpose Equipment and Advanced Processing Technology, Ministry of Education and Zhejiang Province, Zhejiang University of Technology, Hangzhou 310023, China
[c] College of Materials Science and Engineering, Zhejiang University of Technology, Hangzhou 310014, China
[d] State Key Laboratory of Nonlinear Mechanics (LNM), Institute of Mechanics, Chinese Academy of Sciences, Beijing 100190, China

GRAPHICAL ABSTRACT

Here the tubular architecture in poly(vinylidene fluoride-trifluoroethylene) (P(VDF-TrFE)) composite film has been constructed with modified halloysite nanotubes (HNTs) to accomplish an effective diffusion of matter and energy units under high electric field. The energy density in 2 wt% composite achieves 7.0 J/cm^3 with charge-discharge efficiency of 77% at 300 MV/m based on the efficient transportation of ions within hollow nanotubular structure.

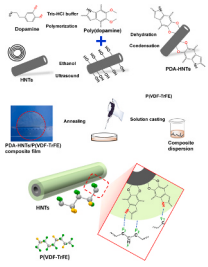

ARTICLE INFO

Keywords:
Polymer composite
Halloysite nanotube
Dielectric property
Polarization
Energy density

ABSTRACT

Dielectric polymer capacitors with high power density as well as efficient charge-discharge rate are widely investigated in past decades. The development of polymer film with large electric capability has become the research topic for the energy storage of advanced power equipment. Here the tubular architecture in poly(vinylidene fluoride-trifluoroethylene) (P(VDF-TrFE)) composite film has been constructed with modified halloysite nanotubes (HNTs) to accomplish an effective diffusion of matter and energy units under high electric field. The nanotube surface was functionalized with poly(dopamine) (PDA) in tris-buffer solution to improve the compatibility with fluoropolymer. The energy capability of P(VDF-TrFE) composite film is enhanced owing to the large content of electroactive phase and interfacial polarization. The dielectric constant in 4 wt% PDA-HNTs/P(VDF-TrFE) film is 34.1 at 100 Hz, and the energy density in 2 wt% composite achieves 5.6 J/cm^3 with charge-discharge efficiency of 74% at 250 MV/m based on the efficient transportation of ions within hollow nanotubular structure. This work delivers a simple method to construct the efficient diffusion route in polymer dielectrics for film capacitor with high energy density and cycle efficiency.

* Corresponding author at: College of Mechanical Engineering, Zhejiang University of Technology, Hangzhou 310023, China.
** Corresponding authors.
E-mail addresses: hpwu@zjut.edu.cn (H. Wu), lilong@lnm.imech.ac.cn (L. Li), huy19@zjut.edu.cn (H. Ye).

https://doi.org/10.1016/j.colsurfa.2021.126993
Received 15 April 2021; Received in revised form 3 June 2021; Accepted 5 June 2021
Available online 9 June 2021

1. Introduction

Polymer film has been proposed as one of most potential candidates in electrostatic capacitors due to superior breakdown feature and large power density with efficient charge-discharge conversion [1–4]. Low energy density of polymer capacitor becomes key issue for the application in the commercial power supply. The electric energy density of polymer film that could be stored is determined by the dielectric constant and breakdown strength [5–7]. Polymer composite combining large dielectric constant and low energy dissipation factor is urgently demanded for the next-generation film capacitor.

The PVDF-based polymer with large permittivity exhibits potential application in electrostatic capacitor with outstanding energy capability [1,5]. To further increase the dielectric constant of fluoropolymer, the inclusion of high-*k* ferroelectric ceramics has been identified as an effective strategy. The common high-*k* fillers, such as $BaTiO_3$, Pb$(Zr_xTi_{1-x})O_3$ and $KTa_{1-x}Nb_xO_3$ have been incorporated into polymer composite to achieve large permittivity [8–11]. However, the presence of inorganic ceramics would inevitably compromise the mechanical characteristics of polymer films [12]. The defects and voids at the interface of composite account for poor breakdown strength due to huge difference in permittivity and conductivity between organic polymer and inorganic component [13]. Thus, the surface functionalization of filler has been proposed to diminish the mismatching phenomena at interfacial region in fluoropolymer composite. The low-surface-energy molecules (e.g. silane coupling agents) and core-shell structure were utilized to achieve the uniform distribution of fillers in polymer matrix [14,15]. PVDF composite embedding with core-shell $BaTiO_3$@Al_2O_3 particles exhibited high discharged electrical capacity, and the energy density of 2.5 vol% nanocomposite film reached the peak of 6.2 J/cm^3 at 380 MV/m, which was ascribed to the improved interfacial region in fluoropolymer composite [16].

The permittivity and polarized response of composite are also dependent on the geometry of nanofiller that would also determine the energy capability of resultant polymer film [12]. Compared with spherical particles, polymer composite incorporated with one-dimensional nanofillers exhibits superiority in capacitance at low fraction, which is attributed to the decrease of field distortion internal polymer host [15,17–21]. The skeleton of halloysite nanotubes (HNTs) is shaped by the curvature of the layers that is arranged with rolling transformation, resulting from the lateral misfit between adjacent sheets of mineral clay [22]. HNTs present unique two-layered aluminosilicate architecture with different diameters, and the distinctive structure with low concentration of polarized clusters contributes to strong interconnection with polar macromolecular segments [23]. Because of the environmental friendly and economical availability, halloysite clay is suggested as one kind of important components in polymer composites [24,25]. The development of modified HNTs/polymer composite with high dielectric property could expand the applications of polymer dielectrics in electronic devices.

In this work, PDA-HNTs/P(VDF-TrFE) composite comprising with nanotubular architecture was prepared by solution casting method. P(VDF-TrFE) as a typical strong-polarity polymer generates the strong interaction with modified nanotube [26]. Also, the inclusion of PDA-HNTs induces the transition of the β-phase from α-phase, during which the stabilization of electroactive phase is due to the conformable crystal assembling between clay mineral and β-phase in fluoropolymer [27]. The strong interconnection from positive charge methylene of the fluoropolymer and negative charged surface of mineral results in the alignment of polymer segments as the propagated all-*trans* conformation [28,29]. The released energy density of 2 wt% composite film is 5.6 J/cm^3 with efficiency of 74% at 250 MV/m, which is attributed to the combination of high electroactive proportion and large interfacial polarized response. The efficient diffusion in the tubular architecture has been constructed to achieve the improved energy capability in the PDA-HNTs/P(VDF-TrFE) composite for film capacitor.

2. Experimental

2.1. Raw materials

The industrial halloysite was provided by Hebei province as commercial clay minerals. Tris(hydroxymethyl) aminomethane (99%) and the dopamine hydrochloride were purchased from Shanghai J&K Scientific Technology Ltd and Hefei BioBomei Co, respectively. P(VDF-TrFE) resin was bought from Piezotech. The N,N-dimethylformamide (DMF), hydrochloric acid (AR), and sodium hydrate (AR) were provided by Shanghai Lingfeng Co.

2.2. Preparation of PDA-HNTs/P(VDF-TrFE) composite

The solution casting technology has been utilized to prepare the PDA-HNTs/P(VDF-TrFE) composite film. Generally, the pristine HNTs powders were added into dopamine hydrochloric acid solution with 0.01 mol L^{-1} under sonication for 1 h. After washing and drying processes, the functionalized PDA-HNTs were obtained. The PDA-HNTs and P(VDF-TrFE) resin were mixed proportionally in DMF with stirring for 3 h. Finally, the mixture was slowly poured onto a glass plate that was exposed in vacuum oven at 80 °C for 12 h. The free-standing thick composite film was obtained after annealing treatment at 100 °C for 10 h.

2.3. Characterizations of PDA-HNTs

In order to identify the PDA attachment on surface of nanotube, the morphological details were evaluated by TEM with JEM-100CX II system (FEI, USA). The XRD characterization was performed on PNAlytical instrument to estimate the structural pattern of PDA-HNTs. The functionalization of PDA-HNTs surface was also characterized by FTIR with Nicolet 6700.

2.4. Structure and electric property for composite film

The FTIR characterizations of PDA-HNTs/P(VDF-TrFE) films were performed to comprehend the phenomenon of phase transition induced by modified nanotube, and the crystal patterns of composites were recorded by XRD. The cross-sectional morphology of composite was evaluated by the SEM with NanoSEM 450 from FEI. The dielectric spectrum of PDA-HNTs/P(VDF-TrFE) film versus the testing frequency was obtained with the utilization of Agilent 4294A. The hysteresis displacements of composites versus different external voltages were collected with the employment of Radiant Technologies TREK 609B-3-K-CE system.

3. Results and discussion

3.1. Morphology and nanostructure for PDA-HNTs

The polymer composite with outstanding electric energy capability is identified as the next-generation candidate for the film capacitor in advanced power supplies. The diffusion channels for the ions and electron have been constructed in PDA-HNTs/P(VDF-TrFE) composite, in which the shortcut path accounts for the high permittivity and large polarized response under external electric field. The polymer modifier was applied to functionalize the halloysite clay mineral in order to diminish the mismatch of permittivity [30,31]. Here, the PDA-HNTs/fluoropolymer composites were obtained via solution casting technology, and the scheme for the modification of halloysite and preparation of composite is illustrated in Fig. 1. The dopamine was polymerized in tri-HCl buffer with reactions of hydroxyl groups on halloysite surface. The modified HNTs were mixed with P(VDF-TrFE)/DMF dispersion to prepare free-standing composite film with tubular architecture. The thick films with different loadings of

PDA-HNTs were obtained after annealing process. The compatible composite film with high dielectric constant and electric displacement is due to functionalization of surface as well as facile diffusion of ions and electron inside hollow tubular structure.

The surface of HNTs was attached by PDA layer in buffer solution to improve the compatibility between inorganic mineral clay and fluoropolymer. In order to evaluate the modification of organic coating, the morphology of nanotube was characterized by TEM technique, and the results are demonstrated in Fig. 2. It can be observed from Fig. 2a and b that the resultant nanotube exhibits inner caliber of ~15 nm and external diameter of ~60 nm, respectively. Also, the detected thin shell evidences that the modifier layer is attached via reactions with hydroxyl ends on HNTs surface [25]. The presence of hydroxyl group in the HNTs was recorded by FTIR, and the spectra are shown in Fig. 2c. The bending vibration at 694 cm^{-1} is assigned for Si-O group on clay mineral after the modification, plus the absorptions at 1633 cm^{-1} and 1480 cm^{-1} belong to benzene ring with C=C stretching mode, indicating that the PDA segments were grafted successfully on surface of halloysite [17]. The XRD curve of PDA-HNTs is displayed in Supplemental Information Fig S1. The organic coating at the interface increases the compatibility between HNTs and polymer, which provides the foundation for the enhancement of electric property and polarization for polymer composite film.

3.2. The electroactive phase and dielectric property of composite film

The PDA-HNTs/P(VDF-TrFE) film was prepared by common solution casting method. In order to address the structural evolutions caused by the addition of nanotubes, XRD and FTIR characterizations of composites were performed. The XRD results of PDA-HNTs/P(VDF-TrFE) composites are presented in Fig. 3a, and the variation of spacing for composite film is clarified based on diffraction in accordance with Bragg law. Compared with pristine P(VDF-TrFE), the peak at 20.0° for composite becomes sharp, which is due to the transition of P(VDF-TrFE) crystal forms during crystallization of fluoropolymer with the existence of modified nanotube acting as heterogeneous nucleation [32]. PVDF-based composites with kaolinite and montmorillonite were reported with the increase fraction of electroactive phase, which was ascribed to the conversion of polar phase by the conformable crystal assembling between fillers and fluoropolymer. The strong interconnection from positive charge methylene of fluoropolymer and negative surface of mineral contributes to propagation of polymer segments as extended all-*trans* conformation [33,34]. With the incorporation of PDA-HNTs into matrix, the surface of nanotube yields strong interaction with polymer host, which results in the accumulation of polar phase in fluoropolymer. This phenomenon is consistent with the higher melting limit and faster crystallization rate for mineral/polymer composite [35].

FTIR is one of most effective techniques for identifying crystal forms in PVDF-based composite [5,12]. FTIR spectra of pristine P(VDF-TrFE) and its composites have been conducted to estimate the phase transition in fluoropolymer. As shown in Fig. 3b, the P(VDF-TrFE) film exhibits two huge absorptions at 763 and 836 cm^{-1} assigning to α and β-phase, respectively. The large content of β-phase that is ascribed to the combination of thermal annealing effect and strong interconnections between fillers and polymer host is also verified by XRD pattern. The hydrogen bonding interactions are probably generated from the modified HNTs with adjacent fluoropolymer, which accelerates the conversion from nonpolar to electroactive phases during crystallization [33]. The large dielectric constant and low loss are vital parameters that should be concerned to pave the path for applications of polymer dielectrics in film capacitors. The dielectric property of PDA-HNTs/P(VDF-TrFE) composites versus testing frequency are plotted in Fig. 3c and d. The maximum dielectric constant $\varepsilon' = 34.1$ at 100 Hz is reached in 4 wt% composite, which is a great improvement compared with $\varepsilon' = 16.8$ for pure P(VDF-TrFE). Furthermore, the value of dielectric loss (ε'') declines slightly with the applied frequency, which may be resulted

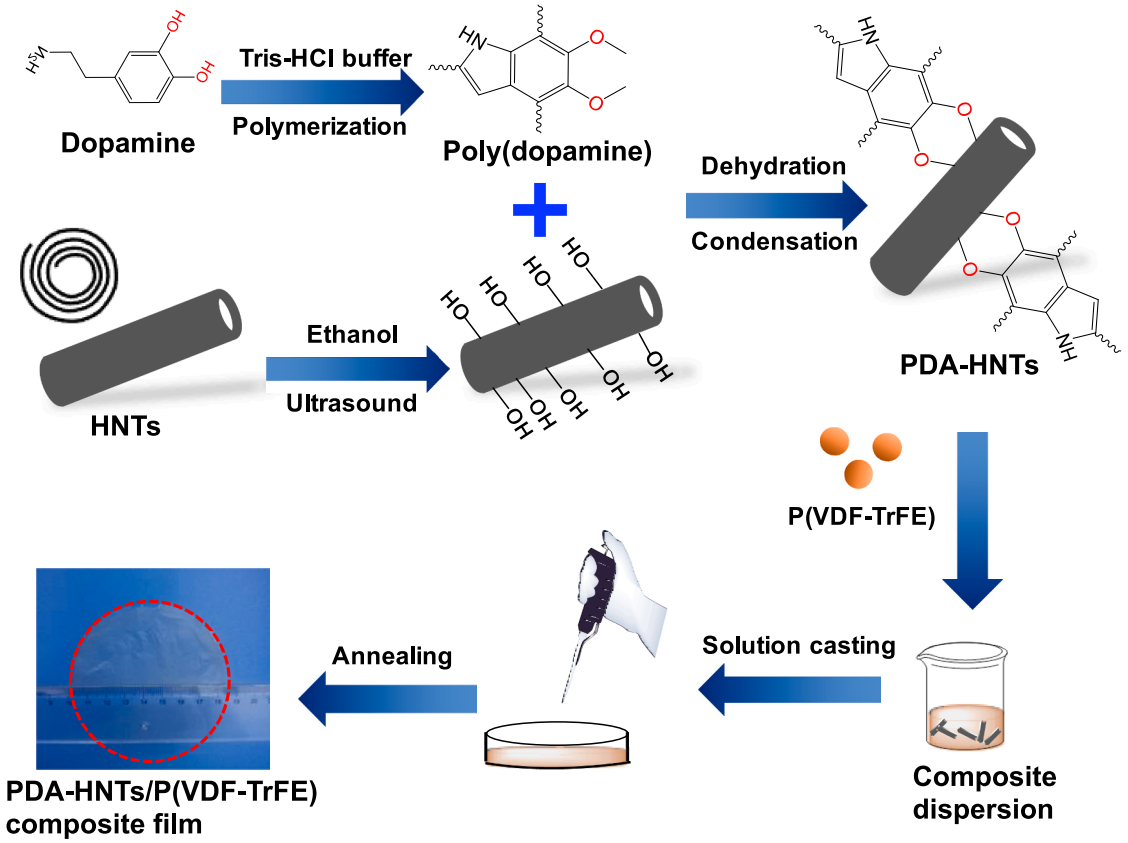

Fig. 1. The modification for HNTs surface and the preparation of PDA-HNTs/P(VDF-TrFE) composite film.

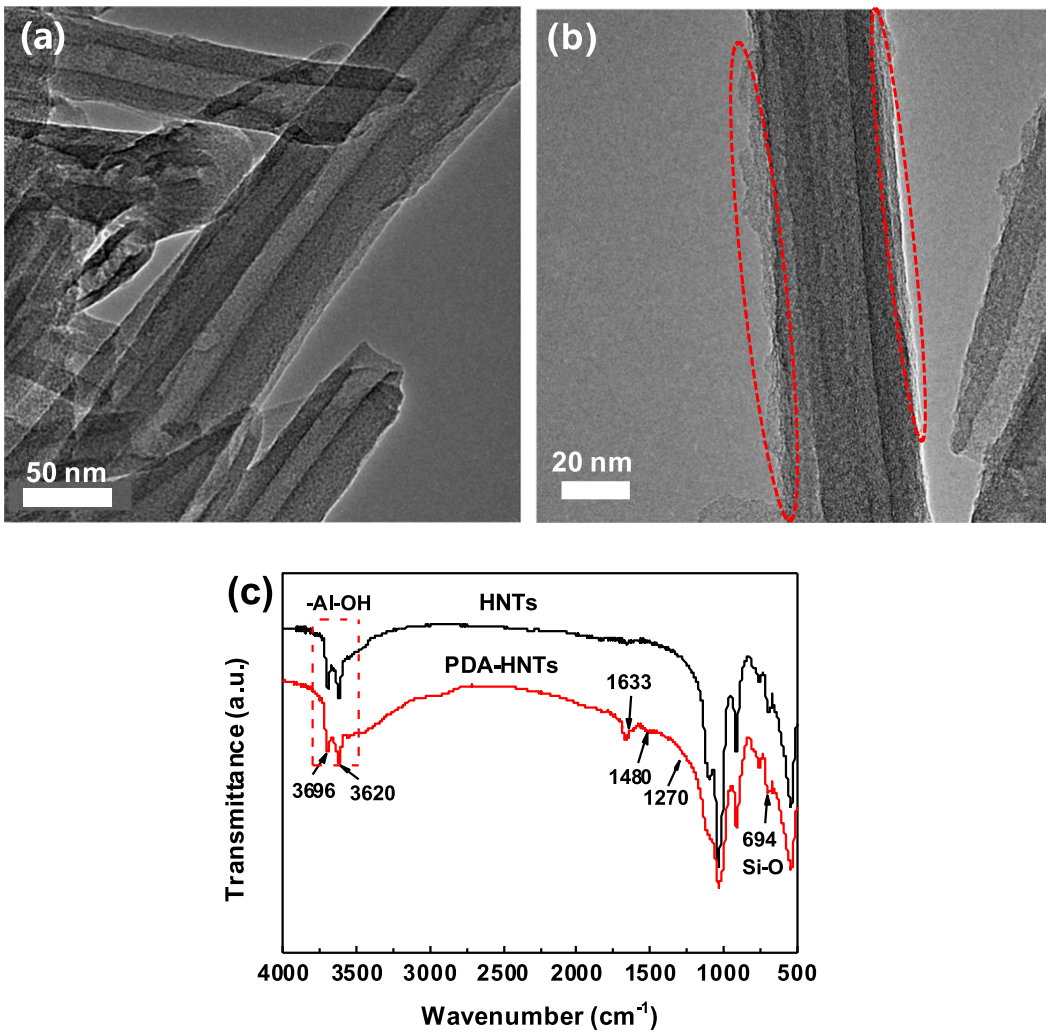

Fig. 2. The morphological and structural characterizations of PDA-HNTs: (a) and (b) TEM images, and (c) FTIR spectra.

from charge mobilization inside P(VDF-TrFE) matrix [12]. The ε" value of composite illustrates huge increase above 10^4 Hz due to the excessive charge polarized interface caused by dipole alignment [36].

3.3. Electric storage property of composite

The hysteresis displacement curves of PDA-HNTs/P(VDF-TrFE) composites versus different electric fields are displayed in Fig. 4. The unipolar loops of fluoropolymer composites with different loadings of PDA-HNTs measured by ferroelectric testing platform are illustrated in Supplemental Information Fig S2. The electric displacement of film rises monotonically with the increasing applied field. The hysteresis loops of pristine P(VDF-TrFE) and 2 wt% composite films are presented in Fig. 4a and b. The dielectric displacement for 2 wt% film is increased compared with pure P(VDF-TrFE) under the identical field. To quantitatively examine the displacement of modified composite, the maximum polarizations and remanent polarizations of films are plotted in Fig. 4c and d, respectively. The peak displacement of 2 wt% composite reaches 6.1 μC/cm^2 at 250 MV/m because of the improved interfacial polarization [29]. Considering the variation of conductivity at the interfacial region and the aggregation of electrical carriers, it's deduced that the factor of breakdown behavior should be concerned in dielectric film capacitor. The feature breakdown strength of PDA-HNTs/P(VDF-TrFE) composite is estimated through Weibull expression (1) [37]:

$$P(E) = 1 - \exp(-(E/E_0)^m) \quad (1)$$

in which $P(E)$ represents the possibility of breakdown failure, E corresponding to experimental breakdown value, E_0 the strength with 63.2% possibility to be catastrophic for the sample, and shape parameter m is applied to evaluate the distribution of collected data. The scatter strength calculated from Weibull equation is demonstrated in Fig. 4e, from which the E_0 for P(VDF-TrFE) composite decreases due to introduction of modified PDA-HNTs in polymer matrix serving as impurity component [38,39].

The polarization behavior of ferroelectric material normally illustrates the non-linear phenomenon under external electric field [40,41]. Generally, the released electric energy density (U_e) by the polymer dielectrics is obtained from *P-E* loop according to the Eq. (2):

$$U_e = \int EdD \quad (2)$$

in which E represents the electric strength and D labels for the polarization. The discharged energy density and total efficiency of composite versus external electric field are shown in Fig. 5. The energy density of polymer film is enhanced with the increasing external field, while the charge-discharge efficiency (η) is reduced, which is probably induced by the large hysteresis under high field. It's suggested that high-*k* inorganic filler is accompanied with large conductive loss that decreases the efficiency during field on-off cycle [42,43]. The discharged energy density U_e = 5.6 J/cm^3 at 250 MV/m is achieved in 2 wt% composite with stored energy percentage η = 74%, which is ascribed to the improved

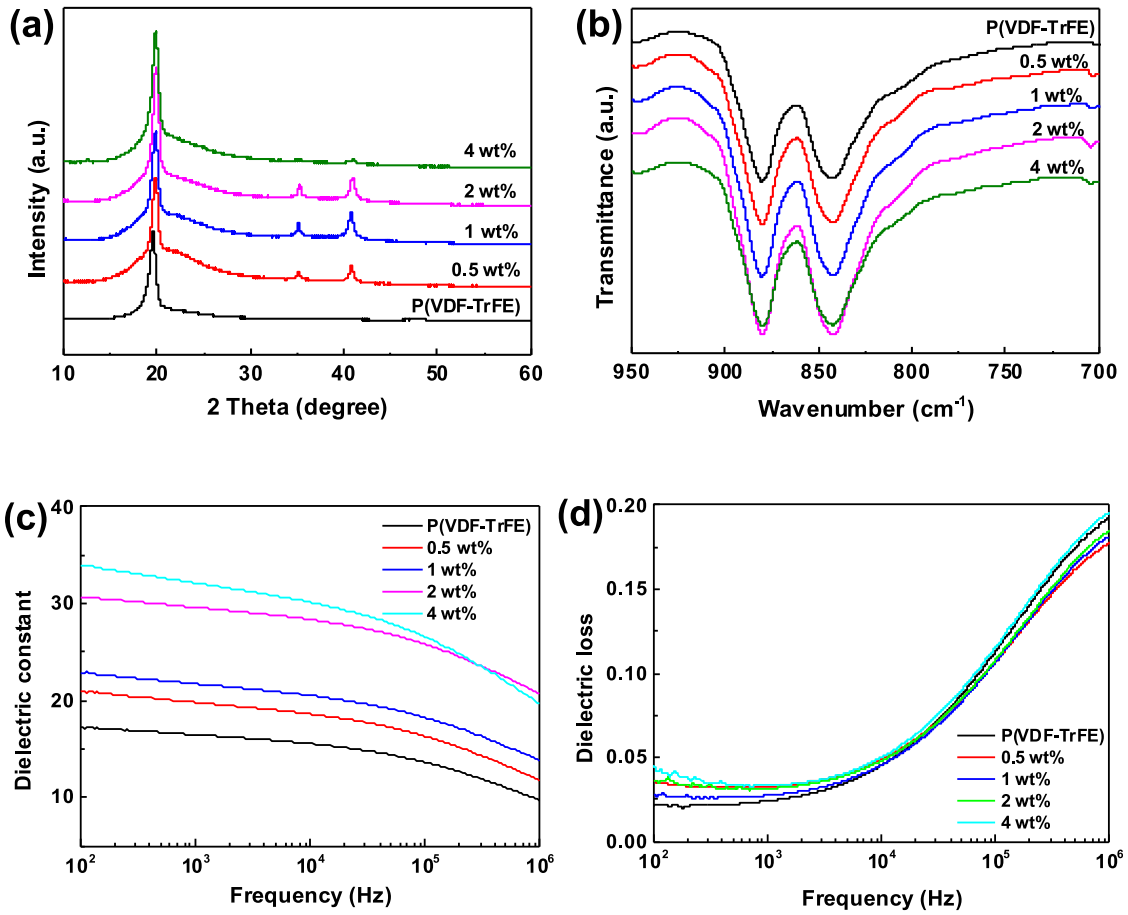

Fig. 3. The structural characterization and dielectric property of PDA-HNTs/P(VDF-TrFE) composite: (a) XRD curves, (b) FTIR spectra, (c) dielectric constant and (d) dielectric loss.

compatible interface after the introduction of modified shell. The SEM images of PDA-HNTs/P(VDF-TrFE) composites are displayed in Supplemental Information Fig. S3, from which it's observed that the modified HNTs are dispersed uniformly in the matrix at low loading. The comparison of electrical energy capability for some fluoropolymer composites is summarized in Table 1. The dielectric composite film with large energy capacity and low power dissipation factor would be fundamental solution for pulse polymer capacitor. The functionalization with organic layer on the surface of clay mineral has been verified as a competitive strategy to develop the polymer composite film.

The external and internal surface of HNTs adsorbs certain amount of oxides and hydroxyl groups that are reacted with PDA to yield irreversible modification on nanotubes, which contributes to strong interconnection with fluoropolymer segments [21]. The interfacial interaction mechanism between PDA-HNTs and P(VDF-TrFE) polymer is illustrated schematically in Fig. 6. In addition, halloysite has one-dimensional structure with large-aspect-ratio hollow architecture that serves as the efficient diffusion for the ion and electron under high external field. The modified nanotube is also proposed as heterogeneous nucleation during the crystallization of P(VDF-TrFE) with the strong interaction between PDA segments and fluoropolymer matrix. The propagation of polymer chain on surface of filler prefers to the formation of polar phase, which increases significantly the dipolar polarization under electric field. The phenomenon of ionic conductance in large-aspect-ratio silicon nitride film capillary device evidenced that the small molecule diffused efficiently inside the tubular skeleton, where the ionic transportation was determined by the surface-charge-governed property [50,51]. The nanotube with large aspect ratio establishes an internal path for the decrease of diffusion track, which results in the capable motions of polar matters. The fixed charge content f inside the channel is described as Eq. (3):

$$f = 2 \times 10^{-3} \frac{\sigma_s}{qN_A h} \tag{3}$$

where σ_s is the surface charge density, q the elementary charge, h the tubular diameter, and N_A represents Avogadro's number [52]. The proton transmission in two-dimensional nanofluidic system with the strong drive force had also verified the diffusion of matter and ions [53]. The molecular dynamics simulation technique was utilized to evaluate the transport performance in 2D system with nano-channels, and the clay minerals were proposed as efficient alternatives to construct the nanofluidic generator with benefit of fast diffusion of ions [54]. The nanofluidic structure was comprised by graphene oxide stacks with layered interval of ~1 nm, in which the efficient diffusion of K^+ and Cl^- ions resulted in high conductivity of fabricated device [55]. The vacant tube is convenient to the effective motion of charge carrier that contributes to polarized behavior of resultant composite. This phenomenon was also proved in porous carbon/cotton supercapacitor with large capacitance based on the diffusion of activated reactions inside tubular structure [56]. The enhancement of capacitance was attributed to the diminished energy barrier for intercalation as well as the effective transportation of lithium-ion in the electrolyte [57]. The interlayer expanded architecture is preferred for the efficient transportation that

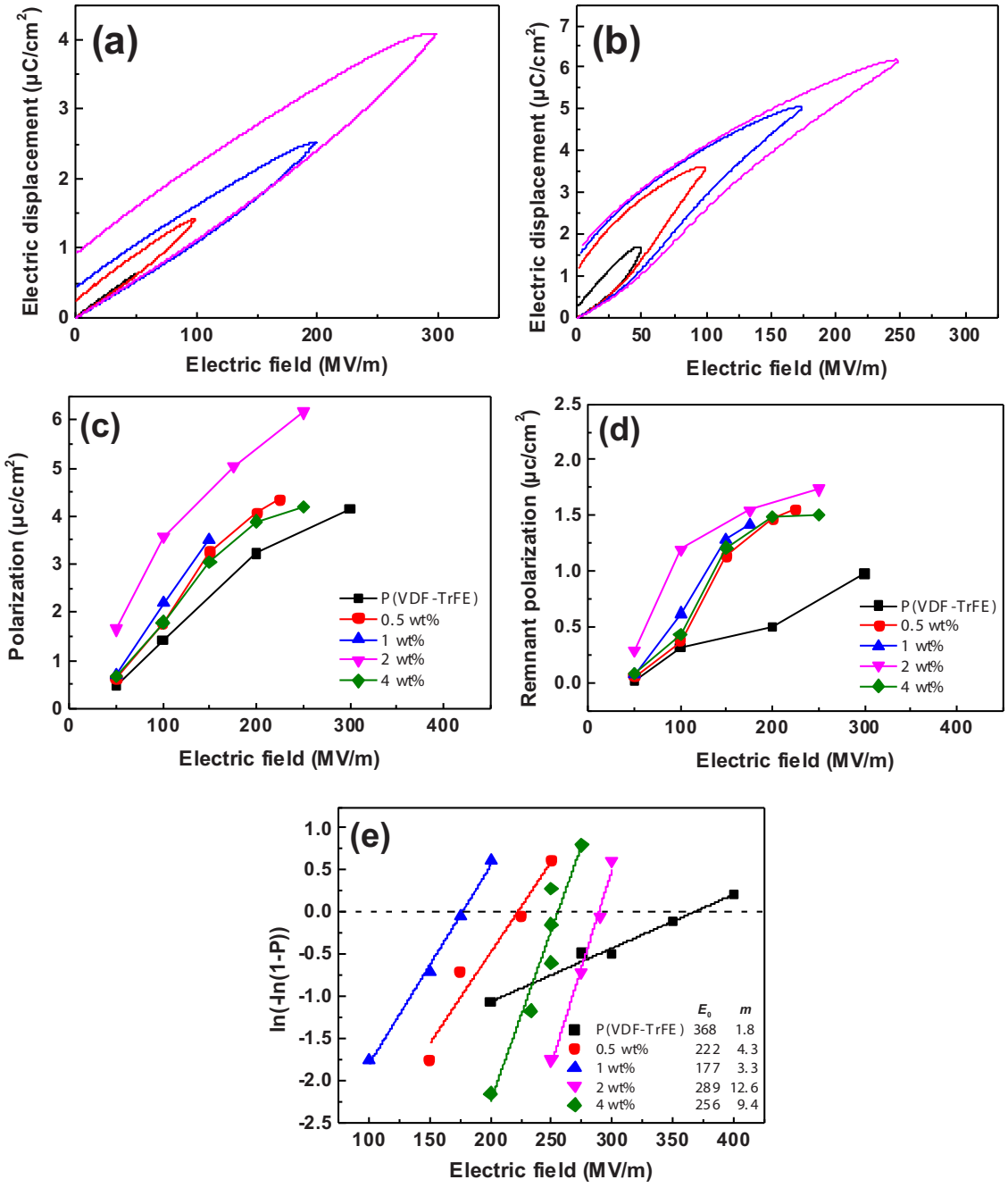

Fig. 4. The electric hysteresis displacements of PDA-HNTs/P(VDF-TrFE) composites: (a) P-E loops for P(VDF-TrFE) film, (b) P-E loops for 2 wt% composite, (c) maximum displacement, (d) the remnant polarization, and (f) Weibull distribution.

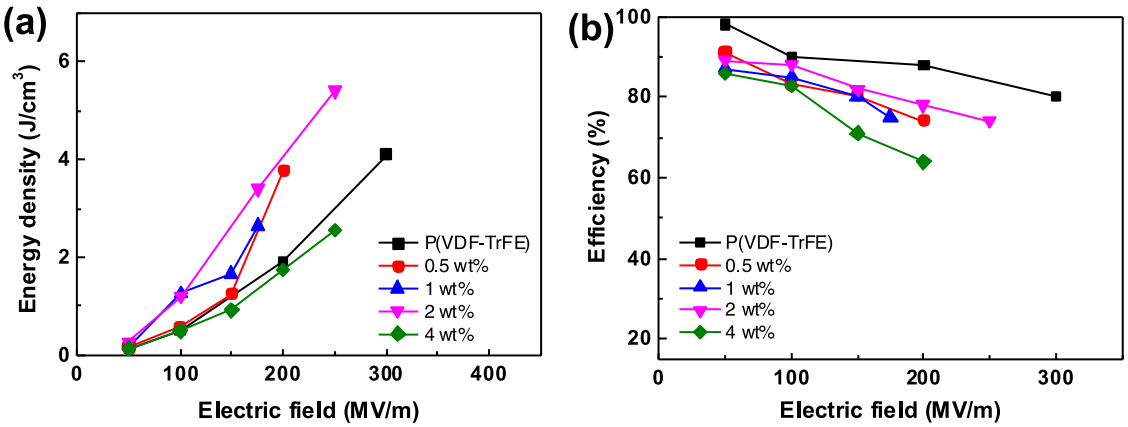

Fig. 5. The energy storage capability of PDA-HNTs/P(VDF-TrFE) composite: (a) energy density, and (b) charge-discharged efficiency. The solid line is drawn to guide eyes.

Table 1
The comparison of energy capability for some fluoropolymer composites from previous reports and this work.

Sample	Loading	ε' (1 kHz)	ε" (1 kHz)	E (MV/m)	U_e (J/cm^3)	η (%)	Ref
PDA-HNTs/P(VDF-TrFE)	2 wt%	15.1	0.06	250	5.6	74	This work
BNNSs/P(VDF-CTFE)	8 wt%	8.7	0.09	325	3	66	[44]
TiO_2/PVDF	18 vol%	18	0.07	225	3.8	78	[45]
$BaTiO_3$ nanowires/P(VDF-HFP)	10 vol%	17	–	200	3.4	57	[46]
TiO_2 nanosheets/PMMA/P(VDF-HFP)	10 wt%	10.5	0.07	400	6.9	63	[47]
$BaTiO_3$@TiO_2@Al_2O_3 nanofiber/PVDF	7.2 vol%	22	0.02	225	3.8	70	[48]
KH590-kaolinite/P(VDF-HFP)	5 vol%	16	0.003	225	3	50	[49]
Halloysite/PVDF	1 wt%	20	0.4	–	–	–	[30]

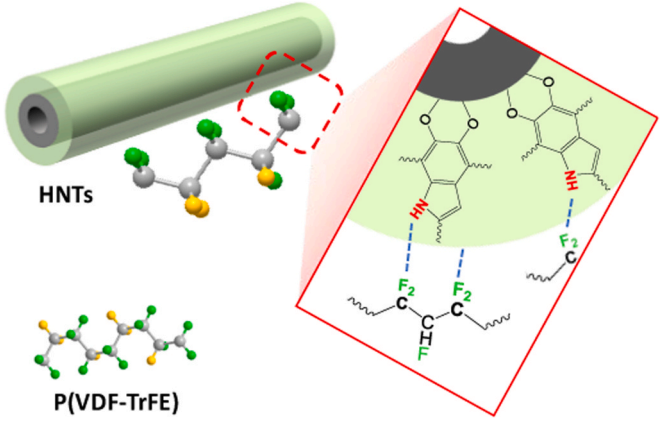

Fig. 6. The schematic view for the interconnection mechanism between modified HNTs and P(VDF-TrFE).

results in the accessible polarized response [58,59]. The functionalization of clay surface is an effectual route to unite the merits of industrial mineral and the advantages of polymer dielectrics. The PDA-HNTs/P(VDF-TrFE) film with large energy density and low power dissipation factor based on interfacial polarization provides solid foundation for applications of polymer film capacitors in electronic devices.

4. Conclusions

The P(VDF-TrFE) composite incorporating with tubular PDA-HNTs has been developed to achieve the improved energy capability. The tubular skeleton with large aspect ratio serves as internal route that accounts for the shortcut of diffusion for polar matters under external field. The energy density in 2 wt% PDA-HNTs/P(VDF-TrFE) composite film achieves 5.6 J/cm^3 with efficiency of 74% at 250 MV/m, which is attributed to the improved compatibility with the interfacial polarization. This work develops the fluoropolymer composite with tubular architecture for the effective motion of polar units, which provides an insight view for the transportation of polarized units in polymer dielectrics under high electric field.

CRediT authorship contribution statement

Huijian Ye and **Huaping Wu** conceived the conceptualization; **Qiangqiang Qian**, **Yufeng Sheng**, and **Xuanhe Zhang** conducted the data curation and investigation; **Long Li** performed some characterizations during revision; **Huijian Ye** and **Lixin Xu** were responsible for the writing-original draft; and all authors were responsible for the writing-review & editing of manuscript.

Declaration of Competing Interest

The authors declare that they have no known competing financial interests or personal relationships that could have appeared to influence the work reported in this paper.

Acknowledgment

The financial supports from the National Natural Science Foundation of China (12002308, 11672269, 51707175), Natural Science Foundation of Zhejiang Province of China (LTZ20E070001, LR20A020002, LZY21E030002) and Department of Education of Zhejiang Province (Y202043208) are appreciated.

Appendix A. Supporting information

Supplementary data associated with this article can be found in the online version at doi:10.1016/j.colsurfa.2021.126993.

References

[1] C. Ribeiro, C.M. Costa, D.M. Correia, J. Nunes-Pereira, J. Oliveira, P. Martins, R. Goncalves, V.F. Cardoso, S. Lanceros-Mendez, Electroactive poly(vinylidene fluoride)-based structures for advanced applications, Nat. Protoc. 13 (2018) 681–704.

[2] M. Li, H. Wondergem, M.J. Spijkman, K. Asadi, I. Katsouras, P.W.M. Blom, D.M. de Leeuw, Revisiting the δ-phase of poly(vinylidene fluoride) for solution-processed ferroelectric thin films, Nat. Mater. 12 (2013) 433–438.

[3] B. Chu, X. Zhou, K. Ren, B. Neese, M. Lin, Q. Wang, F. Bauer, Q.M. Zhang, A dielectric polymer with high electric energy density and fast discharge speed, Science 313 (2006) 334–336.

[4] K. Zou, Y. Dan, Y. Yu, Y. Zhang, Q. Zhang, Y. Lu, H. Huang, X. Zhang, Y. He, Flexible dielectric nanocomposites with simultaneously large discharge energy density and high energy efficiency utilizing (Pb,La)(Zr,Sn,Ti)O3 antiferroelectric nanoparticles as fillers, J. Mater. Chem. A 7 (2019) 13473–13482.

[5] N. Meng, X. Ren, G. Santagiuliana, L. Ventura, H. Zhang, J. Wu, H. Yan, M.J. Reece, E. Bilotti, Ultrahigh β-phase content poly(vinylidene fluoride) with relaxor-like ferroelectricity for high energy density capacitors, Nat. Commun. 10 (2019) 4535.

[6] R.P. Nie, Y. Li, L.C. Jia, J. Lei, H.D. Huang, Z.M. Li, PVDF/PMMA dielectric films with notably decreased dielectric loss and enhanced high-temperature tolerance, J. Polym. Sci. Part B Polym. Phys. 57 (2019) 1043–1052.

[7] T. Zhang, X. Zhao, C. Zhang, Y. Zhang, Y. Zhang, Y. Feng, Q. Chi, Q. Chen, Polymer nanocomposites with excellent energy storage performances by utilizing the dielectric properties of inorganic fillers, Chem. Eng. J. 408 (2021), 127314.

[8] L. Wu, K. Wu, C. Lei, D. Liu, R. Du, F. Chen, Q. Fu, Surface modifications of boron nitride nanosheets for poly(vinylidene fluoride) based film capacitors: advantages of edge-hydroxylation, J. Mater. Chem. A 7 (2019) 7664–7674.

[9] G. Chen, W. Yang, J. Lin, X. Wang, D. Li, Y. Wang, M. Liang, W. Ding, H. Li, Q. Lei, Geometrical shape adjustment of $KTa_{0.5}Nb_{0.5}O_3$ nanofillers for tailored dielectric properties of $KTa_{0.5}Nb_{0.5}O_3$/PVDF composite, J. Mater. Chem. C 5 (2017) 8135–8143.

[10] J. Chen, Y. Li, Y. Wang, J. Dong, X. Xu, Q. Yuan, Y. Niu, Q. Wang, H. Wang, Significantly improved breakdown strength and energy density of tri-layered polymer nanocomposites with optimized graphene oxide, Compos. Sci. Technol. 186 (2020), 107912.

[11] B. Liu, M. Yang, W.Y. Zhou, H.W. Cai, S.L. Zhong, M.S. Zheng, Z.M. Dang, High energy density and discharge efficiency polypropylene nanocomposites for potential high-power capacitor, Energy Storage Mater. 27 (2020) 443–452.

[12] X. Huang, B. Sun, Y. Zhu, S. Li, P. Jiang, High-k polymer nanocomposites with 1D filler for dielectric and energy storage applications, Prog. Mater. Sci. 100 (2019) 187–225.

[13] J.K. Tseng, K. Yin, Z. Zhang, M. Mackey, E. Baer, L. Zhu, Morphological effects on dielectric properties of poly(vinylidene fluoride-co-hexafluoropropylene) blends and multilayer films, Polymer 172 (2019) 221–230.

[14] Y. Cui, Y. Feng, T. Zhang, C. Zhang, Q. Chi, Y. Zhang, X. Wang, Q. Chen, Q. Lei, Excellent energy storage performance of ferroconcrete-like all-organic linear/ferroelectric polymer films utilizing interface engineering, ACS Appl. Mater. Interfaces 12 (2020) 56424–56434.

[15] H. Chu, C. Fu, X. Wu, Z. Tan, J. Qian, W. Li, X. Ran, W. Nie, Enhancing released electrical energy density of poly(vinylidene fluoride-co-trifluoroethylene)-graft-poly(methyl methacrylate) via the pre-irradiation method, Appl. Surf. Sci. 465 (2019) 643–655.

[16] M.W. Yao, S.Y. You, Y. Peng, Dielectric constant and energy density of poly (vinylidene fluoride) nanocomposites filled with core-shell structured $BaTiO_3$@Al_2O_3 nanoparticles, Ceram. Int. 43 (2017) 3127–3132.

[17] P. Hu, S. Gao, Y. Zhang, L. Zhang, C. Wang, Surface modified $BaTiO_3$ nanoparticles by titanate coupling agent induce significantly enhanced breakdown strength and larger energy density in PVDF nanocomposite, Compos. Sci. Technol. 156 (2018) 109–116.

[18] J. Wang, Y. Xie, J. Lin, Z. Zhang, Y. Zhang, Towards high efficient nanodielectrics from linear ferroelectric P(VDF-TrFE-CTFE)-g-PMMA matrix and exfoliated mica nanosheets, Appl. Surf. Sci. 469 (2019) 437–445.

[19] C. Xu, L. Yuan, G. Liang, A. Gu, Building a poly(epoxy propylimidazolium ionic liquid)/graphene hybrid through (Pi cation)-Pi interaction for fabricating high-k polymer composites with low dielectric loss and percolation threshold, J. Mater. Chem. C 4 (2016) 3175–3184.

[20] H.Y. Chu, C. Fu, J.J. Xu, X.H. Ran, Carbon-doped inorganic nanoassemblies as fillers to tailor the dielectric and energy storage properties in polymer-based nanocomposites, Mater. Des. 188 (2020), 108486.

[21] S. Chen, G. Meng, B. Kong, B. Xiao, Z. Wang, Z. Jing, Y. Gao, G. Wu, H. Wang, Y. Cheng, Asymmetric alicyclic amine-polyether amine molecular chain structure for improved energy storage density of high-temperature crosslinked polymer capacitor, Chem. Eng. J. 387 (2020), 123662.

[22] X. Wan, Y. Zhan, G. Zeng, Y. He, Nitrile functionalized halloysite nanotubes/poly (arylene ether nitrile) nanocomposites: interface control, characterization, and improved properties, Appl. Surf. Sci. 393 (2017) 1–10.

[23] X. Zhou, Q. Zhang, R. Wang, B. Guo, Y. Lvov, G.H. Hu, L. Zhang, Preparation and performance of bio-based carboxylic elastomer/halloysite nanotubes nanocomposites with strong interfacial interaction, Compos. Part A-Appl. Sci. Manuf. 102 (2017) 253–262.

[24] Y. Dong, J. Marshall, H.J. Haroosh, S. Mohammadzadehmoghadam, D. Liu, X. Qi, K.T. Lau, Polylactic acid (PLA)/halloysite nanotube (HNT) composite mats: Influence of HNT content and modification, Compos. Part A-Appl. Sci. Manuf. 76 (2015) 28–36.

[25] M. Liu, Z. Jia, D. Jia, C. Zhou, Recent advance in research on halloysite nanotubes-polymer nanocomposite, Prog. Polym. Sci. 39 (2014) 1498–1525.

[26] D.N. Elumalai, J. Tully, Y. Lvov, P.A. Derosa, Simulation of stimuli-triggered release of molecular species from halloysite nanotubes, J. Appl. Phys. 120 (2016), 134311.

[27] Y. Chen, X. Tang, J. Shu, X. Wang, W. Hu, Q.D. Shen, Crosslinked P(VDF-CTFE)/PS-COOH nanocomposites for high-energy-density capacitor application, J. Polym. Sci. Part B Polym. Phys. 54 (2016) 1160–1169.

[28] P. Martins, C.M. Costa, M. Benelmekki, G. Botelho, S. Lanceros-Mendez, On the origin of the electroactive poly (vinylidene fluoride) β-phase nucleation by ferrite nanoparticles via surface electrostatic interactions, CrystEngComm 14 (2012) 2807–2811.

[29] P. Martins, A.C. Lopes, S. Lanceros-Mendez, Electroactive phases of poly (vinylidene fluoride): determination, processing and applications, Prog. Polym. Sci. 39 (2014) 683–706.

[30] C.W. Tang, B. Li, L. Sun, B. Lively, W.H. Zhong, The effects of nanofillers, stretching and recrystallization on microstructure, phase transformation and dielectric properties in PVDF nanocomposites, Eur. Polym. J. 48 (2012) 1062–1072.

[31] P. Thakur, A. Kool, B. Bagchi, S. Das, P. Nandy, Enhancement of β phase crystallization and dielectric behavior of kaolinite/halloysite modified poly (vinylidene fluoride) thin films, Appl. Clay Sci. 99 (2014) 149–159.

[32] D. Shah, P. Maiti, E. Gunn, D.F. Schmidt, D.D. Jiang, C.A. Batt, E.P. Giannelis, Dramatic enhancements in toughness of polyvinylidene fluoride nanocomposites via nanoclay-directed crystal structure and morphology, Adv. Mater. 16 (2004) 1173–1177.

[33] V. Sencadas, P. Martins, A. Pitães, M. Benelmekki, J.L.G. Ribelles, S. Lanceros-Mendez, Influence of ferrite nanoparticle type and content on the crystallization kinetics and electroactive phase nucleation of poly(vinylidene fluoride), Langmuir 27 (2011) 7241–7249.

[34] J. Chen, X. Wang, X. Yu, L. Yao, Z. Duan, Y. Fan, Y. Jiang, Y. Zhou, Z. Pan, High dielectric constant and low dielectric loss poly(vinylidene fluoride) nanocomposites via a small loading of two-dimensional Bi_2Te_3@Al_2O_3 hexagonal nanoplates, J. Mater. Chem. C 6 (2018) 271–279.

[35] L. Priya, J.P. Jog, Poly(vinylidene fluoride)/clay nanocomposites prepared by melt intercalation: crystallization and dynamic mechanical behavior studies, J. Polym. Sci. Part B Polym. Phys. 40 (2002) 1682–1689.

[36] J. Belovickis, M. Ivanov, Š. Svirskas, V. Samulionis, J. Banys, A.V. Solnyshkin, S. A. Gavrilov, K.N. Nekludov, W. Shvartsman, M.V. Silibin, Dielectric, ferroelectric, and piezoelectric investigation of polymer-based P(VDF-TrFE) composites, Phys. Status Solidi (b) 255 (2018), 1700196.

[37] V. Tomer, E. Manias, C.A. Randall, High field properties and energy storage in nanocomposite dielectrics of poly(vinylidene fluoride-hexafluoropropylene), J. Appl. Phys. 110 (2011), 044107.

[38] P. Kim, N.M. Doss, J.P. Tillotson, P.J. Hotchkiss, M.J. Pan, S.R. Marder, J. Li, P. J. Calame, J.W. Perry, High energy density nanocomposites based on surface-modified BaTiO3 and a ferroelectric polymer, ACS Nano 3 (2009) 2581–2592.

[39] L. Yang, Q. Zhao, Y. Hou, R. Sun, M. Cheng, M. Shen, S. Zeng, H. Ji, J. Qiu, High breakdown strength and outstanding piezoelectric performance in flexible PVDF based percolative nanocomposites through the synergistic effect of topological-structure and composition modulations, Compos. Part A-Appl. Sci. Manuf. 114 (2018) 13–20.

[40] S. Luo, Y. Shen, S. Yu, Y. Wan, W.-H. Liao, R. Sun, C.-P. Wong, Construction of a 3D-BaTiO3 network leading to significantly enhanced dielectric permittivity and energy storage density of polymer composites, Energy Environ. Sci. 10 (2017) 137–144.

[41] F. Liu, Q. Li, J. Cui, Z. Li, G. Yang, Y. Liu, L. Dong, C. Xiong, H. Wang, Q. Wang, High-energy-density dielectric polymer nanocomposites with trilayered architecture, Adv. Funct. Mater. 27 (2017), 1606292.

[42] Z. Li, G.M. Treich, M. Tefferi, C. Wu, S. Nasreen, S. Scheirey, R. Ramprasad, G. Sotzing, Y. Cao, High energy density and high efficiency all-organic polymers with enhanced dipolar polarization, J. Mater. Chem. A 7 (2019) 15026–15030.

[43] H. Luo, X. Zhou, C. Ellingford, Y. Zhang, S. Chen, K. Zhou, D. Zhang, C.R. Bowen, C. Wan, Interface design for high energy density polymer nanocomposites, Chem. Soc. Rev. 48 (2019) 4424–4465.

[44] Y. Xie, J. Wang, Y. Yu, W. Jiang, Z. Zhang, Enhancing breakdown strength and energy storage performance of PVDF-based nanocomposites by adding exfoliated boron nitride, Appl. Surf. Sci. 440 (2018) 1150–1158.

[45] L. Yao, Z. Pan, S. Liu, J. Zhai, H.H. Chen, Significantly enhanced energy density in nanocomposite capacitors combining the TiO_2 nanorod array with poly (vinylidene fluoride), ACS Appl. Mater. Interfaces 8 (2016) 26343–26351.

[46] G. Wang, X. Huang, P. Jiang, Tailoring dielectric properties and energy density of ferroelectric polymer nanocomposites by high-k nanowires, ACS Appl. Mater. Interfaces 7 (2015) 18017–18027.

[47] Y. Zhu, H. Yao, P. Jiang, J. Wu, X. Zhu, X. Huang, Two-dimensional high-k nanosheets for dielectric polymer nanocomposites with ultrahigh discharged energy density, J. Phys. Chem. C 122 (2018) 18282–18293.

[48] Z. Pan, J. Zhai, B. Shen, Multilayer hierarchical interfaces with high energy density in polymer nanocomposites composed of $BaTiO_3$@TiO_2@Al_2O_3 nanofibers, J. Mater. Chem. A 5 (2017) 15217–15226.

[49] Y. Zhang, T. Zhang, L. Liu, Q. Chi, C. Zhang, Q. Chen, Y. Cui, X. Wang, Q. Lei, Sandwich-structured PVDF-based composite incorporated with hybrid Fe_3O_4@BN nanosheets for excellent dielectric properties and energy storage performance, J. Phys. Chem. C 122 (2018) 1500–1512.

[50] B. Radha, A. Esfandiar, F.C. Wang, A.P. Rooney, K. Gopinadhan, A. Keerthi, A. Mishchenko, A. Janardanan, P. Blake, L. Fumagalli, M. Lozada-Hidalgo, S. Garaj,

S.J. Haigh, I.V. Grigorieva, H.A. Wu, A.K. Geim, Molecular transport through capillaries made with atomic-scale precision, Nature 538 (2016) 222–225.
[51] J.J. Shao, K. Raidongia, R.A. Koltonow, J. Huang, Self-assembled two-dimensional nanofluidic proton channels with high thermal stability, Nat. Commun. 6 (2015) 7602.
[52] L.J. Cheng, L.J. Guo, Rectified ion transport through concentration gradient in homogeneous silica nanochannels, Nano Lett. 7 (2007) 3165–3171.
[53] X. Zhang, Q. Wen, L. Wang, L. Ding, J. Yang, D. Ji, Y. Zhang, L. Jiang, W. Guo, Asymmetric electrokinetic proton transport through 2D nanofluidic heterojunctions, ACS Nano 13 (2019) 4238–4245.
[54] J. Gao, Y. Feng, W. Guo, L. Jiang, Nanofluidics in two-dimensional layered materials: Inspirations from nature, Chem. Soc. Rev. 46 (2017) 5400–5424.
[55] K. Raidongia, J. Huang, Nanofluidic ion transport through reconstructed layered materials, J. Am. Chem. Soc. 134 (2012) 16528–16531.
[56] W. Jiang, L. Li, J. Pan, A.R. Senthil, X. Jin, J. Cai, J. Wang, X. Liu, Hollow-tubular porous carbon derived from cotton with high productivity for enhanced performance supercapacitor, J. Power Sources 438 (2019), 226936.
[57] H. Dai, R. Zhang, M. Zhong, S. Guo, Effects of the inherent tubular structure and graphene coating on the lithium ion storage performances of electrospun NiO/Co3O4 nanotubes, J. Phys. Chem. C 124 (2020) 143–151.
[58] Y. Cui, W. Liu, W. Feng, Y. Zhang, Y. Du, S. Liu, H. Wang, M. Chen, J. Zhou, Controlled design of well-dispersed ultrathin MoS2 nanosheets inside hollow carbon skeleton: toward fast potassium storage by constructing spacious “houses” for K ions, Adv. Funct. Mater. 30 (2020), 1908755.
[59] J.K. Kim, K.E. Lim, W.J. Hwang, S.K. Park, Hierarchical tubular-structured MoSe2 nanosheets/N-doped carbon nanocomposite with enhanced sodium storage properties, ChemSusChem 13 (2020) 1546–1555.